

PILE FOUNDATION RESPONSE DUE TO SOIL LATERAL SPREADING DURING HYOGO-KEN NANBU EARTHQUAKE

Kohji KOYAMADA, Yuji MIYAMOTO and Yuji SAKO

*Kobori Research Complex, Kajima Corporation, Tokyo, Japan
Email: koyamada@krc.kajima.co.jp*

ABSTRACT

Pile foundations near the shoreline were severely damaged during the Hyogo-ken Nanbu Earthquake, January 17, 1995. This was obviously caused by soil liquefaction. The objective of this study is to investigate the responses of pile foundations due to liquefaction induced lateral spreading. Earthquake response analyses of a structure on pile foundations are conducted using a numerical model taking into account the effect of excess pore water pressure. Observed strong motion in a borehole array at Port Island is employed as the input motion to the soil-pile foundations-structure system. As a result, it is found that soil responses near the shoreline are greatly affected by liquefaction induced lateral spreading, and that large pile bending moments are mainly caused by kinematic interactions at the pile head and at GL-19m, the lower boundary of the reclaimed soil, and that the damaged mechanism of pile foundations varies greatly with distance from the shoreline.

KEYWORDS

Hyogo-ken Nanbu Earthquake; soil liquefaction; lateral spreading; pile foundations response; pile bending moments; kinematic interaction; earthquake response analysis

1. INTRODUCTION

Pile foundations near the shoreline of the reclaimed area were severely damaged during the Hyogo-ken Nanbu Earthquake, January 17, 1995. Damage investigations [1] have shown that not only PC piles and PHC piles but also RC piles and steel pipe piles were damaged due to the lateral spreading. Many subsequent reports have suggested that the pile damage is closely related to the large soil deformation due to the lateral spreading [2], [3]. However, the mechanism of pile damage due to the lateral soil spreading has not been completely clarified. In this study, earthquake response analyses of a structure supported on pile foundations are conducted in order to verify the effects of lateral soil spreading on pile foundation responses. The analyses are conducted in the following two stages. Firstly, soil responses are calculated by a 2D-FEM effective stress analysis taking into account the lateral spreading. Then, the structure response is calculated by the numerical model taking into account the effect of the excess pore water pressure. The analysis results clarify that the response and the damage mechanism of the pile foundations vary with distance from the shoreline.

2. ANALYSIS METHOD AND MODEL

The soil response analysis is conducted by a 2D-FEM effective stress analysis method using the computer program "FLIP" [4]. The computer program is a time history response analysis program and employs a multiple shear mechanism model for the strain dependency of soil stiffness and Iai-Towhata model for evaluating the generation of excess pore water pressure. Figure 1 shows the analysis model and Table 1 shows the soil constants at Port Island. The depth of a quay wall is set at 8m and the influence of seawater is ignored. The quay wall is a steel sheet pile wall, modeled as a linear beam element. The backfill sand and rubble mound are modeled as linear solid elements with shear wave velocities of 200m/s and 300m/s, respectively. The boundary condition of the bottom is set as fixed and that of the side is set as a viscous damper. The observed strong motion in the borehole array at Port Island is employed as the input motion for the analysis. The shear wave velocities of each layer are based on the results of a geological survey [5]. The shear wave velocity for a

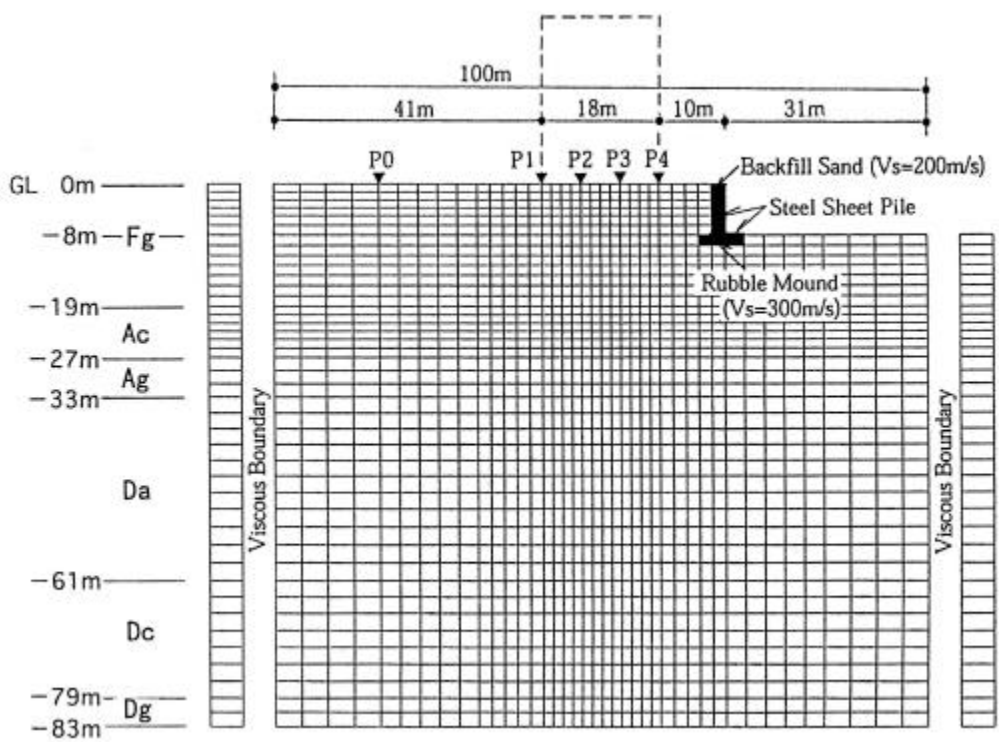


Figure 1 Analysis Model for 2D-FEM Effective Stress Analysis

Table 1 Soil Constants at Port Island

Depth	Soil Type*	Density (tf/m ³)	S-wave Velocity (m/s)	Internal Friction Angle(°)	Cohesion (tf/m ²)	Mesh Size
▼GL-2.5m (Water Table)	Fg	1.80	140	36	-	1.25m × 4
GL-19m						1.52m × 5
						1.60m × 4
GL-27m	Ac	1.70	180	-	18.0	1.30m × 4 1.40m × 2
GL-33m	Ag	1.87	245	40	-	2.00m × 3
GL-61m	Da	1.87	305	40	-	2.40m × 5 2.50m × 2
		1.87	350	40	-	2.75m × 4
GL-79m	Dc	1.62	303	-	34.0	2.50m × 2 2.60m × 5
GL-83m	Dg	1.90	320	40	-	2.00m × 2

* Fg: Filling Gravel, Ac: Alluvial Clay, Ag: Alluvial Gravel
Da: Diluvial Alternate Layer, Dc: Diluvial Clay, Dg: Diluvial Gravel

Parameters of FLIP

GL-0m~GL-19m

W1= 3.0, S1=0.005, P1=0.5, P2=0.6, C1=1.00, $\phi_p=28^\circ$

GL-27m~GL-33m

W1=16.5, S1=0.005, P1=0.5, P2=0.8, C1=3.43, $\phi_p=28^\circ$

reclaimed layer (Fg) is set at 140m/s in the middle of the layer [6]. The nonlinear properties of the soil are based on laboratory test results [7]. Figure 2 shows the liquefaction curves of the reclaimed layer (Fg) and the alluvial gravel (Ag). These curves are based on laboratory tests [8].

The objective structure for the analyses is an eight-story reinforced concrete building (2 × 3 span) and its first natural period is about 0.5 seconds. Table 2 shows the analysis constants of the structure model. The structure is supported by 12 reinforced concrete piles (3 × 4) of diameter 1.4m and length 38m. The distance between the building (hereafter, S1-bldg) and the shoreline is set 10m. The dotted line in Figure 1 shows the position of the S1-bldg and the symbols P1-P4 show the positions of the pile foundations.

Seismic response analyses of the structure supported on the pile foundations are conducted using a beam-interaction spring model, as shown in Figure 3 [9]. The superstructure is idealized by a one-stick model with lumped masses and beam elements. The pile foundations are idealized by a 4-stick model with lumped masses and beam elements with three piles perpendicular to the direction of the vibration. The lumped masses of the pile foundations are connected to the free field soil through lateral and shear interaction springs. A linear rotational spring related to the axial stiffness of the piles is also incorporated at the pile head.

The initial values of the lateral and shear interaction soil springs of pile groups are obtained using Green's functions by ring loads in a layered stratum [10] and they are equalized to four pile foundations. The soil springs are modified in accordance with the relative displacements between soils and pile foundations and with the generation of excess pore water pressures.

The relationship between the story shear force Q and the shear deformation of the superstructure is modeled by applying the tri-linear model [6]. The nonlinear properties of the pile foundations are incorporated into the relationships between the bending moments M and the curvature ϕ , and the relationships are evaluated by a static push-over analysis with Fiber-Model [11] and modeled by applying the tri-linear model.

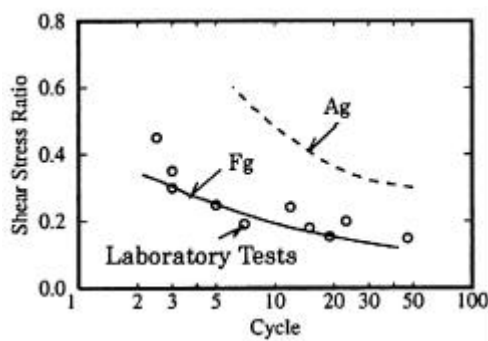


Table 2 Analysis Constants of Structure Model

Floor	Height (m)	Weight (tf)	EI (tf·m ²)	GA (tf)
8	3.2	225	5.5E+8	3.5E+5
7	3.2	250	7.2E+8	3.6E+5
6	3.2	250	7.6E+8	3.6E+5
5	3.2	250	7.8E+8	3.7E+5
4	3.2	250	7.7E+8	3.7E+5
3	3.2	250	7.6E+8	3.8E+5
2	3.2	250	7.9E+8	4.1E+5
1	3.6	255	8.0E+8	5.9E+5
F		420		

Figure 2 Liquefaction Curve of Reclaimed Layer

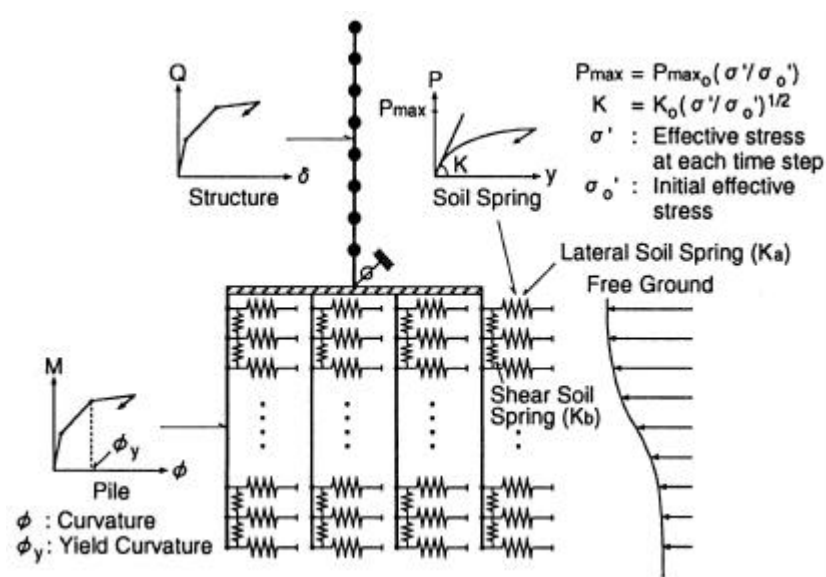


Figure 3 Numerical Model of Soil-Pile-Structure System for Response Analysis

3. SOIL RESPONSE DUE TO LATERAL SPREADING

Figure 4 shows the maximum soil responses at the site at distances 10m (P4), 28m (P1) and 53m (P0) from the shoreline. The excess pore water pressures (hereafter EPWP) in the reclaimed layer above GL-19m reach to the initial effective stress σ'_0 , indicating that complete liquefaction occurs in the layer. The maximum accelerations de-amplify in the reclaimed layer because of the liquefaction. These soil response tendencies are almost the same, regardless of the distance from the shoreline. The maximum relative displacements vary with distance from the shoreline. Those at the ground surface become large for sites close to the shoreline, and those of sites P0, P1 and P4 are about 50cm, 70cm and 140cm, respectively.

Figure 5 shows the time histories of the relative displacements and excess pore water pressure ratios (hereafter

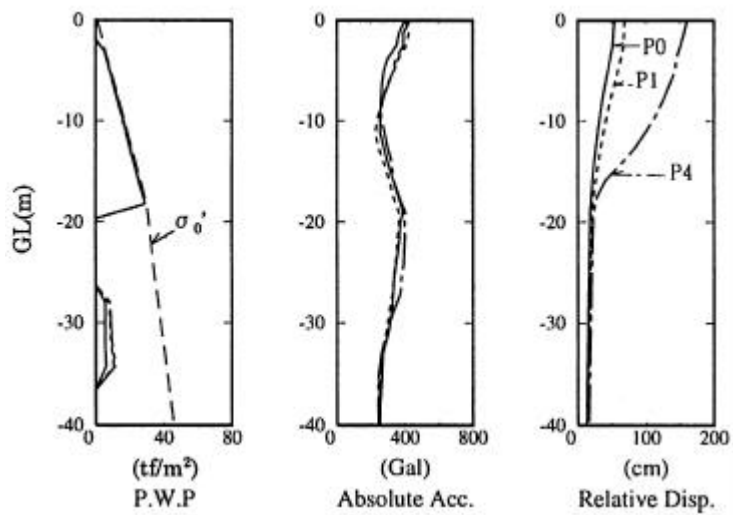


Figure 4 Maximum Distributions of Soil Responses

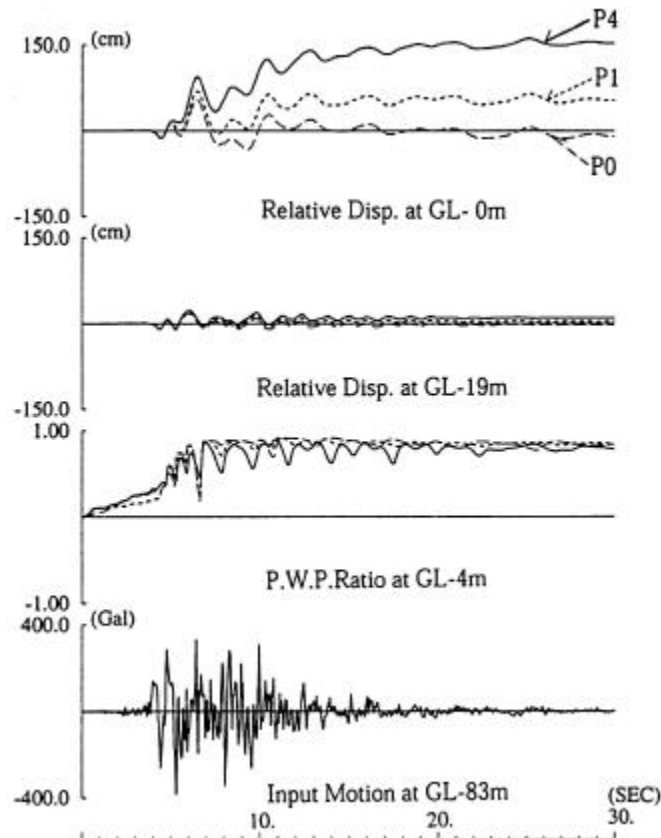


Figure 5 Time Histories of Soil Responses

EPWPR). EPWPRs are the ratios of excess pore water pressures to initial effective stress. The relative displacements at GL-19m, the lower boundary of the reclaimed layer, are almost the same, regardless of the distance from the shoreline, while those at the ground surface vary greatly with distance from the shoreline. The relative displacements increase as the sites become closer to the shoreline. The differences between the relative displacements are shown, especially after the occurrence time of the maximum input acceleration (6.5 seconds). The time histories of the EPWPRs indicate that liquefaction occurred at the time 6.5 seconds. After that time, effective stress recoveries are found in the time histories at all sites. This is because of the cyclic mobility phenomena occurring in the reclaimed layer.

Figure 6 shows the deformation of the soil near the shoreline at two different times, 6.5 seconds and 15 seconds. At the time 6.5 seconds, the reclaimed layer above GL-19m deformed toward the seaside. At the time 15 seconds, only a part of the reclaimed layer near the shoreline deformed toward the seaside due to lateral spreading.

Figure 7 shows the distribution of maximum and residual displacements. In this analysis, both the maximum and the residual displacements at the shoreline reach about 200cm. Both displacements reduce with distance from the shoreline, and the residual displacements disappear at about 50m from the shoreline. The distribution of the residual displacements coincides with the investigation results conducted by Ishihara et al. in Port Island [12].

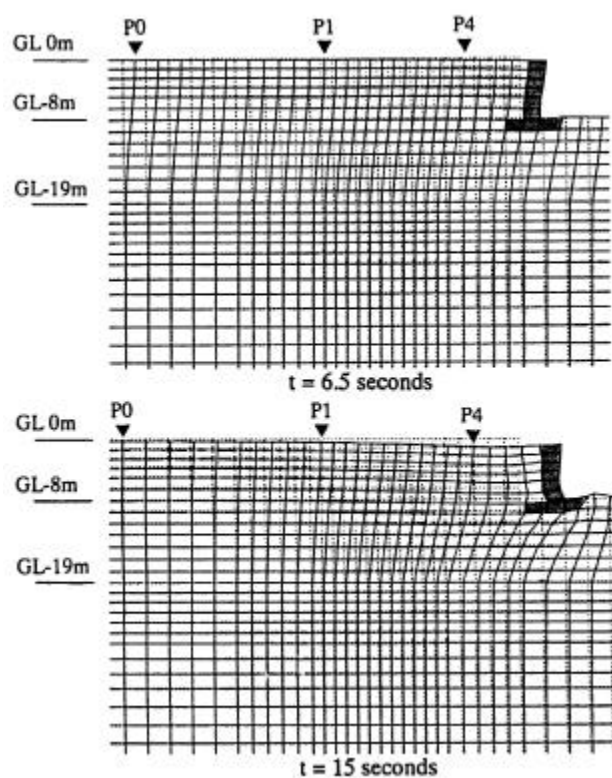


Figure 6 Deformation of Soil near Shoreline

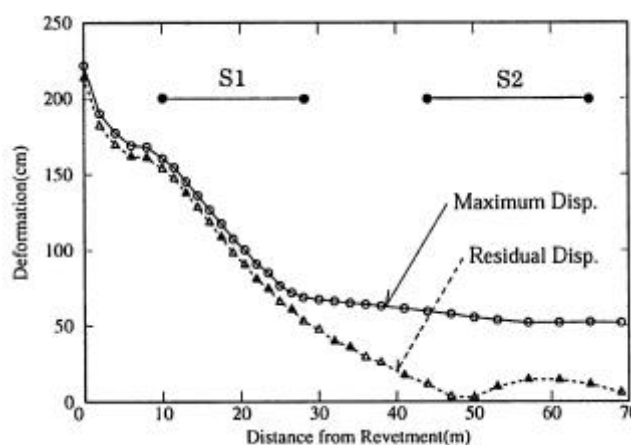


Figure 7 Maximum and Residual Displacements at Ground Surface

4. PILE RESPONSE DUE TO LATERAL SPREADING

Response analyses of the pile foundation are conducted using three models. This is done in order to verify the effect of connecting pile heads with a base mat, and the effect of the inertial forces of the superstructure on the pile responses. Figure 8 shows the schema of the three models. In Case-1 the analyses are carried out for the model in which the pile heads of the four piles are not connected with a base mat, but the rotational deformations of the pile heads are fixed. In Case-2 the analyses are carried out for the model in which the pile heads of the four piles are connected with a base mat without a superstructure. In Case-3 the analyses are carried out for the model including the superstructure.

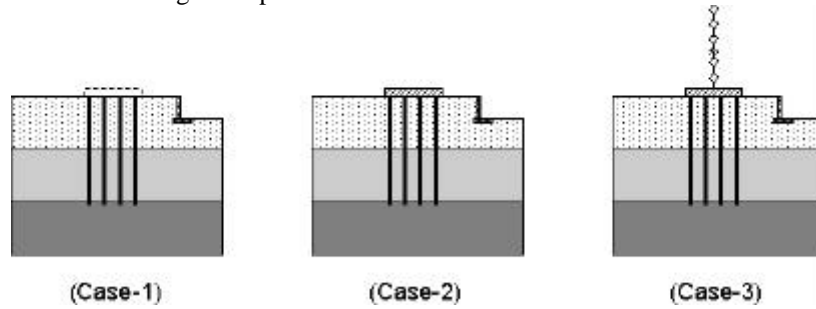


Figure 8 Schema of Models for Pile Response Analysis

4.1 Differences of Pile Responses with Distance from Shoreline:

Pile responses of the building (S1-bldg) near the shoreline are compared with those of the building (S2-bldg) 44m from the shoreline. Pile foundations of the S1-bldg are called Pile-1, 2, 3 and 4 and those of the S2-bldg are called Pile-1', 2', 3' and 4' from the landside, respectively. Pile responses are compared by the analysis results in Case-3.

Figure 9 shows the maximum pile bending moments, the relative pile displacements and the pile ductility ratios. The ductility ratios are evaluated as the ratios of the maximum curvature to the yield point of the tri-linear type

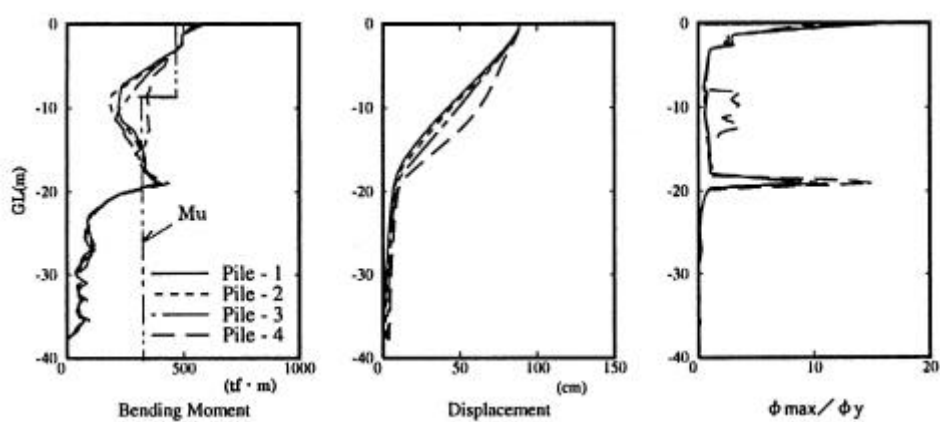


Figure 9 Maximum Pile Responses of S1-bldg in Case-3

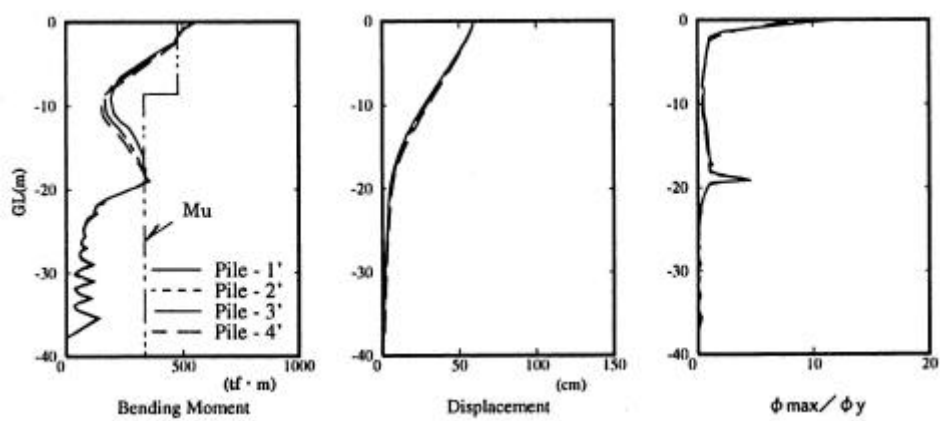


Figure 10 Maximum Pile Responses of S2-bldg in Case-3

hysteresis loop. The maximum bending moments are large at the pile head and at the lower boundary of reclaimed layer (GL-19m), and they reach the ultimate moments M_u of the concrete. In addition, the bending moments of Pile-4 are large at GL-10m and the moment distribution of Pile-4 is different from those of the other pile foundations. The relative pile displacements are amplified from GL-19m to the pile head, and those at the pile heads reach about 90cm. The displacement distributions of Pile-1, 2 and 3 change almost linearly in the reclaimed layer, while those of Pile-4 swell at GL-10m. The pile ductility ratios are large at the pile head, and at GL-19m those of Pile-4 are also large at GL-10m. The pile ductility ratios at the pile head are almost the same, regardless of the position of the pile foundation. However, those at GL-19m for Pile-4 are larger than those for the other piles.

Figure 10 shows the maximum pile responses of S2-bldg. The pile bending moments are large at the pile head and at GL-19m, reaching the ultimate moment M_u of the concrete. The pile displacements are amplified from GL-19m to the pile head, reaching about 60cm at the pile head. The pile ductility ratios are large at the pile head and at GL-19m, as for the pile bending moments. The maximum response distributions of Pile-1', 2', 3' and 4' are almost the same, regardless of the position of the pile foundation. The maximum pile displacement responses and ductility ratios of Pile-1', 2', 3' and 4' are smaller than those of Pile-1, 2, 3 and 4.

This clarifies that the pile responses of the building near the shoreline vary with pile foundations distance from the shoreline. However, the pile responses of the building far from the shoreline are almost the same, regardless of pile position. These analytical results coincide with the damage pattern of the pile foundations during the Hyogo-ken Nanbu Earthquake indicated by Tokimatsu et al. [13].

4.2 Effects on Pile responses of Connecting Pile heads with Base Mat:

Figure 11 shows the maximum pile responses of Pile-1 and Pile-4 in Case-1. The pile displacements are amplified corresponding to the soil displacements in the reclaimed layer, those at the pile head of Pile-1 and Pile-4 reaching about 60cm and 120cm, respectively. The pile bending moments of both Pile-1 and Pile-4 are large at the pile head and at GL-19m, and those of Pile-4 are also large at GL-10m, where the reclaimed layer protruded toward the sea due to lateral spreading. The pile ductility ratios of both Pile-1 and Pile-4 are large at the pile head and at GL-19m as the bending moments, and the maximum ductility ratios of Pile-4 are larger than those of Pile-1.

Figure 12 shows the maximum pile responses of Pile-1 and Pile-4 in Case-2. The pile displacements at the pile

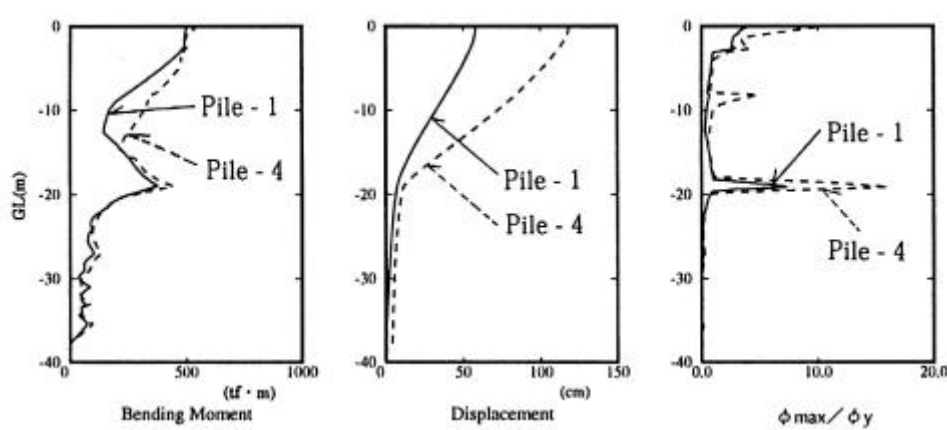


Figure 11 Maximum Pile Responses of S1-bldg in Case-1

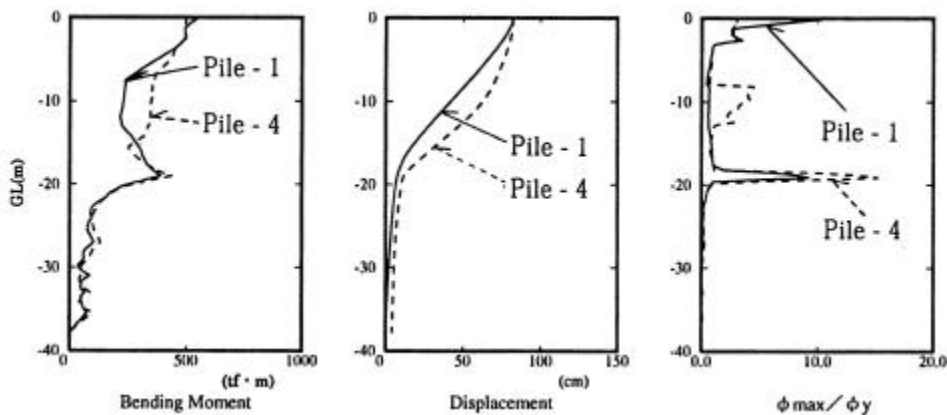


Figure 12 Maximum Pile Responses of S1-bldg in Case-2

heads of both reach about 80cm. When the pile heads are connected with a base mat, the pile displacements of Pile-1 in Case-2 are larger than those in Case-1, while those of Pile-4 in Case-2 are smaller than those in Case-1. The deformation distribution of Pile-1 linearly changes in the reclaimed layer, while those of Pile-4 swell at GL-10m due to lateral spreading. The ductility ratios at the pile head of Pile-1 in Case-2 are larger than those in Case-1. However, the ductility ratios at the pile head of Pile-4 in Case-2 are smaller than those in Case-1, but the range of the damaged area in Case-2 is wider than that in Case-1. The ductility ratios at GL-19m for both Pile-1 and Pile-4 in Case-2 are almost the same as those in Case-1.

It is thus clarified that the pile foundation damage mechanisms vary greatly with distance from the shoreline. The pile foundations on the seaside are pushed out toward the sea by lateral spreading. However, they are pulled back when the pile heads are connected with the pile foundations on the landside. The pile foundations on the landside are pulled toward the sea by the pile foundations on the seaside. Damage to the pile head of the pile foundations on the seaside is suppressed and that of the pile foundations on the landside is increased by connecting pile heads with a base mat.

4.3 Effects on Pile responses of Inertial Force of Superstructure:

Figure 13 shows the maximum bending moments and the maximum ductility ratios of Pile-1 and Pile-4. Figure 14 shows the relationship between the bending moment M and the curvature at the pile head in Case-2 and Case-3. The pile bending moments in Case-2 are almost the same as those in Case-3, because the pile bending moments in both Case-2 and Case-3 reach the ultimate moment of the concrete due to the soil displacements. The pile ductility ratios only at the pile head in Case-2 are different from those in Case-3, and the effects of the inertial force of the superstructure don't reach the deep part of the pile foundations. The ductility ratios at the pile head of Pile-1 and Pile-4 in Case-2 are different, while those in Case-3 are almost the same.

Thus, damage due to soil displacements at the pile head of the pile foundation on the landside increases more than those of the pile foundation on the seaside. However, the damage to the pile foundations on both the seaside and on the landside becomes almost the same due to the inertial force of the superstructure, and the effects of the superstructure on the pile responses don't reach the deep part of the pile foundations.

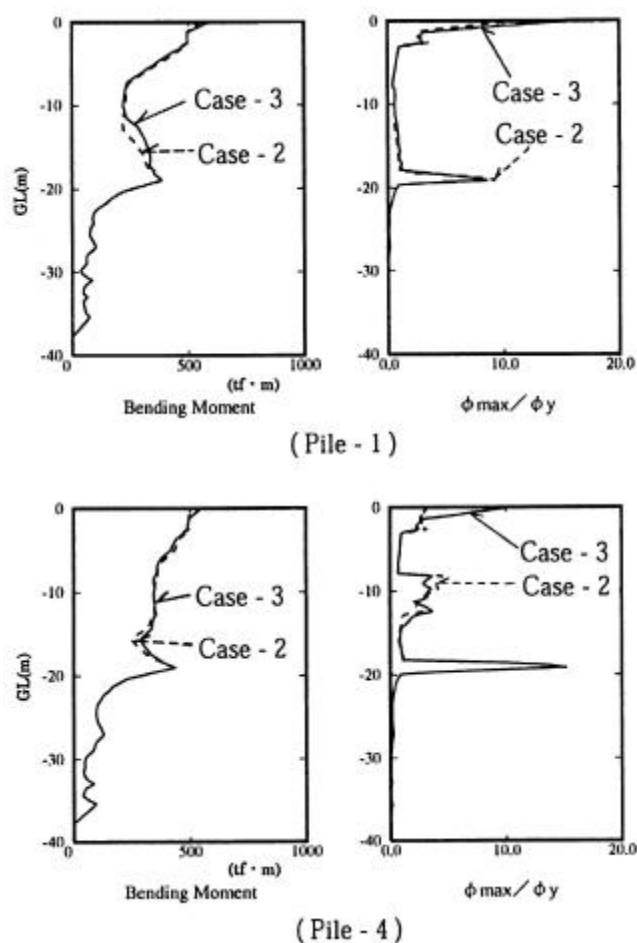


Figure 13 Comparisons of Maximum Pile Responses in Case-2 and Case-3

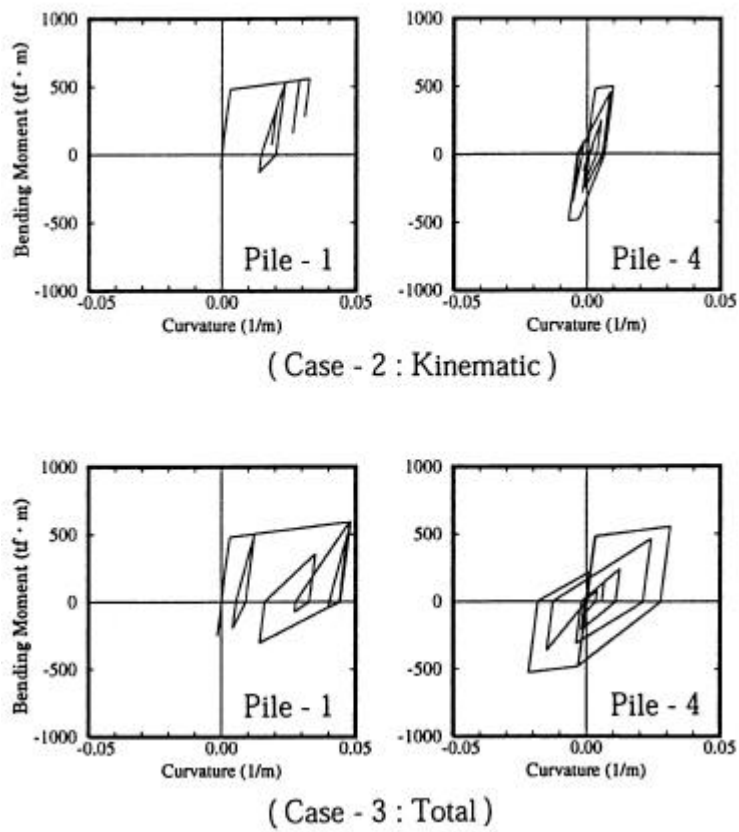


Figure 14 Relationship between Bending Moments M and Curvature at Pile Head

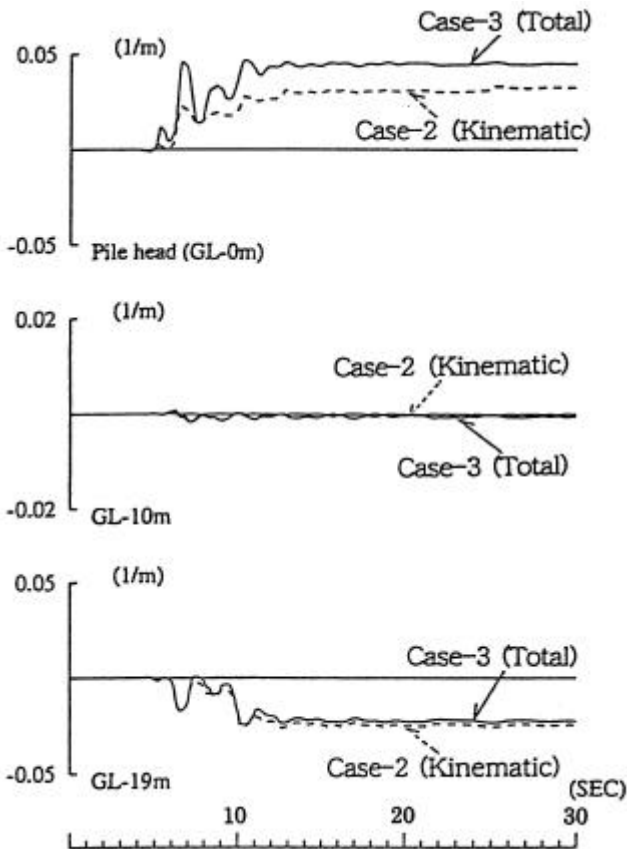


Figure 15 Time Histories of Pile Curvature of Pile-1

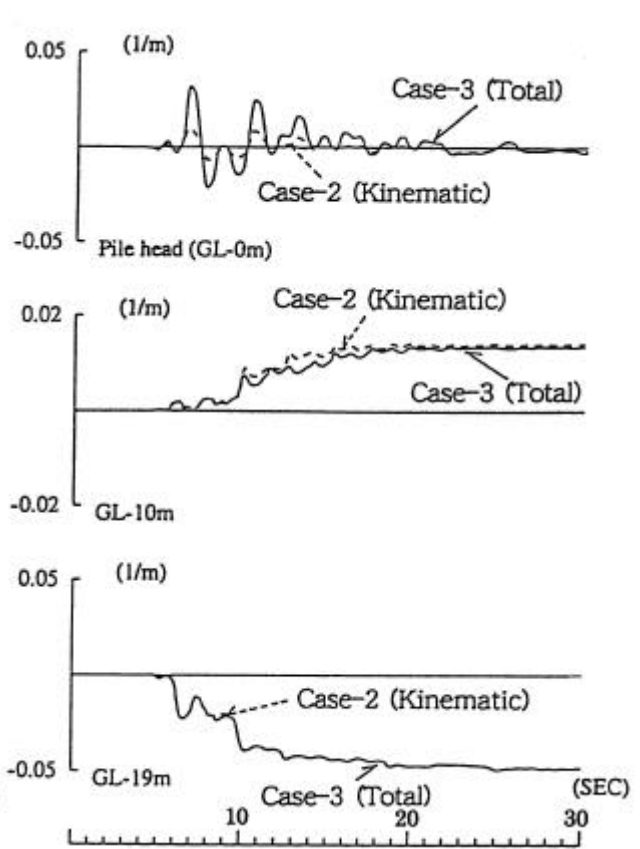


Figure 16 Time Histories of Pile Curvature of Pile-4

Figure 15 shows the time histories of the pile curvatures at the pile head for GL-10m and GL-19m in Case-2 and Case-3 for Pile-1. Figure 16 shows those of Pile-4. The pile curvatures at the pile head and at GL-19m for both Pile-1 and Pile-4 increase at time 6.5 seconds, and the damage to the pile foundations are shown before lateral spreading occurred. Those at the pile head increase at time 10 seconds due to the inertial force of the superstructure, and residual displacements of the pile foundations occur in Pile-1. At GL-19m, the curvatures are large at time 6.5 seconds, and the residual displacements in Pile-4 are larger than those in Pile-1. At GL-10m, the curvatures are small at time 6.5 seconds. However, only the curvature in Pile-4 increases due to lateral spreading.

It is thus clarified that at time 6.5 seconds, when the maximum acceleration of the input motion occur, the damage to the pile head of Pile-1 and Pile-4 was induced by the inertial force of the superstructure and by the soil displacements, and the damage at GL-19m was caused by the soil displacements. The damage to the pile head and GL-19m increases in both Pile-1 and Pile-4, and the damage at GL-10m in Pile-4 increases due to lateral spreading.

5. CONCLUSIONS

In order to verify the mechanism of pile foundation damage due to lateral spreading during the Hyogo-ken Nanbu Earthquake, dynamic response analyses of the structure supported on the pile foundation near the shoreline were conducted. Concluding remarks are as follows.

1. The pile responses of structure near the shoreline vary with distance from the shoreline. However, the pile responses of the structure far from the shoreline are almost the same regardless of the position of the pile foundations. This tendency coincides with the damage pattern of pile foundations due to lateral spreading during the Hyogo-ken Nanbu Earthquake.
2. The damage mechanisms of the pile foundations on the seaside and those on the landside vary with lateral spreading. Damage at the pile head of pile foundations on the seaside is suppressed by pile foundations on the landside. However, damage at the pile head of the pile foundations on the landside is increased by pulling toward the sea by the pile foundation on the seaside.
3. The inertial force of the superstructure affects the response at the pile head of pile foundations on both the seaside and the landside. Damage due to soil displacements at the pile head of the pile foundation on the landside increases more than that on the seaside. However, damage to pile foundations on both the seaside and the landside becomes almost the same by the inertial force of the superstructure, and the effects of the superstructure on the pile responses don't reach the deep part of the pile foundations.
4. Damage at the pile head of pile foundations on both the landside and the seaside is induced by the inertial force of the superstructure and by the soil displacements, while damage at GL-19m is caused by the soil displacements at time 6.5 seconds, when the maximum acceleration of the input motion occurs. Damage at the pile head and at GL-19m increases due to lateral spreading in both Pile-1 and Pile-4, and damage at GL-10m in Pile-4 also increases.

6. REFERENCES

1. Kansai Branch of Architectural Institute of Japan : Report on Case Histories of Damage to Building Foundations in Hyogoken-Nambu Earthquake", Report presented by Committee on Damage to Building Foundations, 1996.7, (in Japanese)
2. The Japanese Geotechnical Society : Proceeding of the Symposium on Lateral Flow and Permanent Deformation of Soil during Earthquake, p.444, 1998.5, (in Japanese)
3. Fukutake, K. and Tokimatsu, K. : Evaluation of Ground Response, Multi-directional nonlinear response of ground and residual deformation, Proc. of the 5th symposium on the dynamic soil-structure interaction, pp. 51-85, (in Japanese)
4. Iai, S., Matsunaga, Y. and Kameoka, T. : Strain Space Plasticity Model for Cyclic Mobility, Soils and Foundation, Vol.32, No.2, pp.1-15, 1992.6
5. Kobe City Development Bureau 1995. Report of Investigation for Liquefaction-induced Large Ground Displacement at Reclaimed Land (Port Island and Rokko Island) (in Japanese).
6. Miyamoto, Y., Sako, Y., Koyamada, K. and Miura, K. : Response of Pile Foundation in Liquefied Soil Deposit during The Hyogo-Ken Nanbu Earthquake of 1995, Journal of Struct. Constr. Eng., AIJ, No.493, pp. 23-30, 1997. 3, (in Japanese)
7. Liu, H., Ichii, K., Morita, T. and Iai, S. : Analysis of Deformation to the Kobe Ohashi Bridge Foundation, Geotechnical Engineering in Recovery from Urban Earthquake Disaster, KIG-Forum, pp. 189-198, 1997

8. Suzuki, Y., Hatanaka, M. and Uchida, A. : Drained and Undrained Shear Strengths of a Gravelly Fill of Weathered Granite from Kobe Port Island, Journal of Struct. Constr. Eng., AIJ, No.498, pp. 67-73, 1997. 8, (in Japanese)
9. Miyamoto, Y., Sako, Y., Kitamura, E. and Miura, K. : Earthquake Response of Pile Foundation in Nonlinear Liquefiable Sand Deposit, Journal of Structural and Construction. Engineering, Architectural Institute of Japan, No. 471, 1995, pp.41-50 (in Japanese)
10. Kausel E. and Peek R. : Dynamic Loads in the Interior of a Layered Stratum- An Explicit Solution", Bulletin of the Seismological Society of America, Vol. 72, 1982, pp. 1459-1481
11. Muto, K., Hisada, T. et al. : Earthquake Resistance Design of a 20 Story Reinforced Concrete Building, 5th World Conference on Earthquake Engineering, pp.1960-1969, 1973
12. Ishihara, K., Yasuda, S. and Nagase, H. : Soil Characteristics and Ground Damage, Soils and Foundations, Special Issue on Geotechnical Aspects on the January 17 1995 Hyogoken-nanbu Earthquake, pp.109-118, 1996
13. Tokimatsu, K. and Oh-oka, H. : Damage to Pile foundations due to lateral Spreading in the Hyogoken-Nambu Earthquake, Proc. of the Symposium on the Lateral Flow and Permanent Deformation of the Soil during the Earthquake, JGS, pp. 287-292, 1998.5, (in Japanese)